A Three-Dimensional Computational Model of the Innate Immune System

Pedro Augusto F. Rocha[1], Micael P. Xavier[1], Alexandre B. Pigozzo[1], Barbara de M. Quintela[1], Gilson C. Macedo[2], Rodrigo Weber dos Santos[1], and Marcelo Lobosco[1]

[1] Graduate Program in Computational Modelling, UFJF
[2] Graduate Program in Biological Science, UFJF

Abstract. The Human Immune System is a complex system responsible for protecting the organism against diseases. Although understanding how it works is essential to develop better treatments against diseases, its complexity makes this task extremely hard. In this work a three-dimensional mathematical and computational model of part of this system, the innate immune system, is presented. The high computational costs associated to simulations lead the development of a parallel version of the code, which has achieved a speedup of about 72 times over its sequential counterpart.

1 Introduction

Computational model is a popular tool to study the behavior of a complex system. This study is done through the simulation of distinct scenarios, which reflects the adjusts done in the parameters of the system under simulation. The results obtained from the computational experiments can then be used by experts to improve their understanding about the system. The system under study is often modelled using an explicit mathematical model, such as an ODE or PDE, although other implicit mathematical models, multi-agent systems or system dynamics, can also be used.

One particular complex system that has benefited from the computational modelling is the Human Immune System (HIS). The HIS is a complex network composed of specialized cells, tissues and organs that is responsible for protecting the organism against diseases caused by pathogenic agents. Although understanding how the HIS is essential to develop better drugs and treatments against diseases, its complexity and the intense interaction among several components, makes this task extremely hard. The use of computational models can help researchers to better understand how it works and their distinct components interacts, allowing them to test a large number of hypotheses in a short period of time.

This paper focus on the modelling of a part of the HIS, the innate immune system. The innate immune system is responsible for the first response against microorganisms or toxins that successfully enter into an organism. The main

B. Murgante et al. (Eds.): ICCSA 2012, Part I, LNCS 7333, pp. 691–706, 2012.

contributions of this paper are the following. First we extend our previous works [1,2] and present a new three-dimensional model of the innate immune system. In particular, the current work focus on the simulation of the immune response to a potent immunostimulant in a microscopic 3D section of tissue, reproducing the initiation, maintenance and resolution of the innate immune response. Second, due to its huge computational cost, we present a parallel version of the 3D code using GPGPUs. A previous attempt to write a parallel version of the one-dimensional version of the code has used OpenMP and MPI[3]. The preliminary GPGPU results have shown that the parallelization process was very successful, yielding speedups up to sixty times.

This paper is organized as follows. In Section 2 the biological background is presented. Section 3 describes the mathematical model used in this work to model the innate immune system, while Section 4 presents its computational implementation and Section 5 presents its numerical results. Section 6 presents the parallelization of the code and the parallel results are presented and discussed in Section 7. The concluding remarks and future works are presented in Section 8.

2 Biological Background

The human body surfaces are protected by epitheliums, that constitutes a physical barrier between the internal and the external environment. However, it can eventually be crossed or settled by pathogens, causing infections. After crossing the epithelium, the pathogens find cells and molecules of the innate immune system that immediately develop an immune response. The strategy of the Human Immune System (HIS) is to keep some resident macrophages, called resting macrophages, into the tissue to look for any signal of invasion. When macrophages find such an invader they become active and ask the help of polymorphonuclear leukocytes (PMNs), such as the neutrophils. The cooperation between macrophages and PMNs is essential to mount an effective defense, because without the macrophages to recruit the PMNs to the location of invasion, the PMNs would circulate indefinitely in the blood vessels, impairing the control of huge infections. For example, protein granules produced by neutrophils contributes to increase the permeability of the walls of the blood vessels, called endothelium, allowing monocytes to enter into the tissues and mature into *resting* macrophages.

This initial response of the HIS starts an inflammatory process that has many benefits on the control of the infection. Besides recruiting cells and molecules of innate immunity from blood vessels to the location of the infected tissue, it increases the lymph flux containing microorganisms and cells that carry antigens to the neighbors lymphoid tissues, where these cells will present the antigens to the lymphocytes and will initiate the adaptive response. The adaptive response is part of the HIS that can adapt to protect the organism against almost any invader. Once the adaptive response is activated, the inflammation also recruits the effector cells of the adaptive immune system to the location of infection.

A component of the cellular wall of Gram-negative bacteria, such as LPS, can trigger an inflammatory response through the interaction with receptors on the surface of some cells. When receptors on the surface of macrophages bind to LPS, the macrophage starts to phagocytosis, degrading the bacteria internally and secreting proteins known as cytokines and chemokines, as well as other molecules.

The resolution of the inflammatory response also includes the production of anti-inflammatory mediators and the apoptosis (or programmed death) of effector cells of the HIS, such as the neutrophils. The anti-inflammatory cytokines are a set of immunoregulatory molecules that control the pro-inflammatory response. The cytokines act together with specific inhibitors and cytokines soluble receptors to regulate the immune response[4]. The main anti-inflammatory cytokines include the antagonist receptor of IL-1 (Interleukin 1), and the cytokines IL-4, IL-6, IL-10, IL-11 e IL-13[4]. The IL-10 is a strong inhibitor of the production of many pro-inflammatory cytokines [5], among them the IL-8 and TNF-α (tumor necrosis factor α) by monocytes [6] and IL-8 by neutrophils [7,8].

The apoptotic cells keep the membrane integrity by a small period of time and so need to be quickly removed to prevent a secondary necrosis and, consequently, the release of cytotoxic molecules that causes inflammation and tissue damage [9]. As a consequence of the phagocytosis of apoptotic cells by macrophages or dendritic cells, these phagocytic cells produces anti-inflammatory cytokines. For example, macrophages secrete TGF-β (transforming growth factor β) that prevents the release of pro-inflammatory cytokines induced by LPS [10]. Also, the binding of the apoptotic cells to macrophage receptor CD36 (cluster of differentiation 36) inhibits the production of pro-inflammatory cytokines such as TNF-α, IL-1β and IL-12 and also increases the secretion of TGF-β and IL-10[11].

3 Mathematical Model

Biological systems span multiple scales from sub-cellular molecular interactions to individual complex organisms. The abstraction level of a model depends on the scale and granularity chosen and it has been a challenge to find a balance between scale, granularity and computational feasibility during the development of a model[12]. As models represent the reality, simplifications maintaining the main components are often used without loosing reliability [13].

This paper models the response of the innate HIS to a potent immunostimulant in a three-dimensional (3D) section of a tissue. In particular, the mathematical model focus on the response to Lipopolysaccharides (LPS), a molecule that can be found in the membrane of bacteria. Previous works [1,2] has reproduced the initiation, maintenance and resolution of the innate immune response in a microscopic one-dimensional (1D) section of a tissue. The new 3D model proposed in this work aims to present more realistic results.

In this work, Partial Differential Equations (PDEs) have been employed to model the spatial and temporal behavior of the following components: LPS (A), macrophages, neutrophils (N), apoptotic neutrophils (ND), pro-inflammatory

cytokines (CH), anti-inflammatory cytokine (CA) and proteins granules (G). In this model, the macrophages are present in two states of readiness: *resting* (MR) and *hyperactivated* (MA). The proinflammatory cytokines, modelled by an unique equation in the model, are TNF-α and IL-8. The anti-inflammatory cytokine modelled is the IL-10. The IL-10 inhibits the activation and effector functions of T cells, monocytes and macrophages [14]. The different subsets of proteins granules [15] released by neutrophils during their extravasation from blood vessel to the tissues are represented by an unique equation.

The main differences related to the previous 1D model [1,2] are the following:

- a larger simulation space is used. An hexahedron is used instead of a line;
- the initial and boundary conditions were adapted for the 3D model;
- the diffusion and chemotaxis were applied in three directions, x, y and z.

3.1 LPS

The equations that models LPS are given by Eq. 1:

$$\begin{cases} maActivation = maActivationRate.MR.A/(1+\theta_{CA}.CA) \\ \frac{\partial A}{\partial t} = -\mu_A A - maActivation - (\lambda_{N|A}N + \lambda_{MA|A}MA).A + D_A \Delta A \\ A(x,y,z,0) = 100 \quad | \quad z \geq 0.9, \frac{\partial A(.,.,.,t)}{\partial n}|_{\partial\Omega} = 0 \end{cases} \tag{1}$$

The term $\mu_A A$ models the decay of LPS, where μ is the rate of decay. The term $maActivation$ models the activation of resting macrophages. This activation occurs when resting macrophages recognizes the LPS. After this recognition, the macrophages phagocyte the LPS. The term $\lambda_{N|A}.N$ models the phagocytosis of LPS by the neutrophils, where $\lambda_{N|A}$ is the rate of this phagocytosis. The term $\lambda_{MA|A}.MA$ models the phagocytosis of LPS by the active macrophages, where $\lambda_{MA|A}$ is the rate of this phagocytosis. The term $D_A \Delta A$ models the LPS diffusion, where D_A is the diffusion coefficient.

3.2 Macrophage

The equations related to resting macrophages (MR) are given by Eq. 2:

$$\begin{cases} Mrpermeability1 = (MrPmax - MrPmin).CH/(CH + keqch) + MrPmin \\ Mrpermeability2 = (MrPmax\_g - MrPmin\_g).G/(G + keq\_g) + MrPmin\_g \\ sourceMR = (Mrpermeability1 + Mrpermeability2). \\ \qquad .(MrmaxTissue - (MR + MA)) \\ \frac{\partial MR}{\partial t} = -\mu_{MR} MR - maActivation + D_{MR} \Delta MR + sourceMR - \\ \qquad -\nabla.(\chi_{MR} MR \nabla CH) \\ MR(x,y,z,0) = 1, \frac{\partial MR(.,.,.,t)}{\partial n}|_{\partial\Omega} = 0 \end{cases} \tag{2}$$

The terms $Mrpermeability1$ and $Mrpermeability2$ model the increase in the endothelium permeability and its effects on the extravasation of monocytes induced by pro-inflammatory citokines and proteins granules, respectively. The permeability of the endothelium of the blood vessels is modelled through a Hill equation [16].

The calculus of $Mrpermeability1$ involves the following parameters: a) $MrPmax$ is the maximum rate of increase in the endothelum permeability induced by the pro-inflammatory cytokine; b) $MrPmin$ is the minimum rate of increase in the endothelum permeability induced by the pro-inflammatory cytokine and c) $keqch$ is the concentration of pro-inflammatory cytokine that exerts 50% of the maximum effect in the increase in the permeability.

The calculus of $Mrpermeability2$ is similar to the calculus of $Mrpermeability1$, except for the parameters that are involved: $MrPmax\_g$, $MrPmin\_g$ and keq_g. The term $sourceMR$ represents the source term of macrophages, which is related to the number of monocytes that will enter into the tissue from the blood vessels. This number depends on the endothelium permeability ($Mrpermeability1 + Mrpermeability2$) and the capacity of the tissue to support the entrance of more monocytes ($MrmaxTissue$).

The term $\mu_{MR}MR$ models the resting macrophage apoptosis, where μ_{MR} is the apoptosis rate. The term $maActivation$, as explained before, models the activation of resting macrophages, representing the number of resting macrophages that are becoming active. The term $D_{MR}\Delta MR$ models the resting macrophage diffusion, where D_{MR} is the diffusion coefficient. The term $\nabla.(\chi_{MR}MR\nabla CH)$ models the resting macrophage chemotaxis, where χ_{MR} is the chemotaxis rate.

After being activated, the macrophages are modelled by the following set of equations (Eq. 3):

$$\begin{cases} \frac{\partial MA}{\partial t} = -\mu_{MA}MA + maActivation + D_{MA}\Delta MA - \nabla.(\chi_{MA}MA\nabla CH) \\ MA(x,y,z,0) = 0, \frac{\partial MA(.,.,.,t)}{\partial n}|_{\partial\Omega} = 0 \end{cases} \tag{3}$$

The term $\mu_{MA}MA$ models the active macrophage apoptosis, where μ_{MA} is the rate of apoptosis. The term $D_{MA}\Delta MA$ models the active macrophage diffusion, where D_{MA} is the diffusion coefficient. The term $\nabla.(\chi_{MA}MA\nabla CH)$ models the active macrophage chemotaxis, where χ_{MA} is the chemotaxis rate.

3.3 Neutrophil

The neutrophil equations (N) are given by Eq. 4.

$$\begin{cases} permeability = (Pmax - Pmin).CH/(CH + keqch) + Pmin \\ sourceN = permeability.(NmaxTissue - N) \\ \frac{\partial N}{\partial t} = -\mu_N N - \lambda_{A|N}A.N + D_N\Delta N + sourceN - \nabla.(\chi_N N\nabla CH) \\ N(x,y,z,0) = 0, \frac{\partial N(.,.,.,t)}{\partial n}|_{\partial\Omega} = 0 \end{cases} \tag{4}$$

The term $((Pmax - Pmin).CH/(CH + Keqch) + Pmin)$ models the increase in the endothelium permeability and its effects on neutrophils extravasation. In this term $Pmax$ represents the maximum rate of increase of endothelium permeability induced by pro-inflammatory cytokines, $Pmin$ represents the minimum rate of increase of endothelium permeability induced by pro-inflammatory cytokines and $keqch$ is the concentration of the pro-inflammatory cytokine that exerts 50% of the maximum effect in the increase of the permeability.

The term $\mu_N N$ models the neutrophil apoptosis, where μ_N is the rate of apoptosis. The term $\lambda_{A|N} A.N$ models the neutrophil apoptosis induced by the phagocytosis, where $\lambda_{A|N}$ represents the rate of this induced apoptosis. The term $D_N \Delta N$ models the neutrophil diffusion, where D_N is the diffusion coefficient. The term $sourceN$ represents the source term of neutrophil, i.e., the number of neutrophils that is entering into the tissue from the blood vessels. This number depends on the endothelium permeability ($permeability$) and on the capacity of the tissue to support the entrance of neutrophils ($NmaxTissue$). It can also represent concentration of neutrophils on blood. In this model we consider $NmaxTissue$ constant over time. The term $\nabla.(\chi_N N \nabla CH)$ models the chemotaxis process of the neutrophils, where χ_N is the chemotaxis rate.

The equations of the apoptotic neutrophil (ND) are given by Eq. 5.

$$\begin{cases} \frac{\partial ND}{\partial t} = \mu_N N + \lambda_{A|N} A.N - \lambda_{ND|MA} ND.MA + D_{ND} \Delta ND \\ ND(x, y, z, 0) = 0, \frac{\partial ND(.,.,.,t)}{\partial n}|_{\partial \Omega} = 0 \end{cases} \tag{5}$$

The terms $\mu_N N$ and $\lambda_{A|N} LPS.N$ were explained previously. The term $\lambda_{ND|MA} ND.MA$ models the phagocytosis of the apoptotic neutrophil carried out by active macrophages, where $\lambda_{ND|MA}$ is the rate of the phagocytosis. The term $D_{ND} \Delta ND$ models the apoptotic neutrophil diffusion, where D_{ND} is the diffusion coefficient.

3.4 Cytokines

The equations related to the model of the pro-inflammatory cytokine (CH) are given by Eq. 6.

$$\begin{cases} \frac{\partial CH}{\partial t} = -\mu_{CH} CH + (\beta_{CH|N}.N + \beta_{CH|MA}.MA).A.(1 - CH/chInf)/ \\ \qquad /(1 + \theta_{CA}.CA) + D_{CH} \Delta CH \\ CH(x, y, z, 0) = 0, \frac{\partial CH(.,.,.,t)}{\partial n}|_{\partial \Omega} = 0 \end{cases} \tag{6}$$

The term $\mu_{CH} CH$ models the pro-inflammatory cytokine decay, where μ_{CH} is the decay rate. The term $\beta_{CH|N}.N$ models the pro-inflammatory cytokine production by the neutrophils, where $\beta_{CH|N}$ is the rate of this production. The term $\beta_{CH|MA}.MA$ models the pro-inflammatory cytokine production by the active macrophages, where $\beta_{CH|MA}$ is the rate of this production. The saturation of this production is calculated by the equation $(1 - CH/chInf)$, where $chInf$ is an estimate of the maximum concentration of pro-inflammatory cytokine supported by the tissue. The production of pro-inflammatory cytokine decreases

when the anti-inflammatory cytokine acts on the producing cells. This influence of the anti-inflammatory cytokine is modelled by the term $1/(1+\theta_{CA}.CA)$. The term $D_{CH}\Delta CH$ models the pro-inflammatory cytokine diffusion, where D_{CH} is the diffusion coefficient.

The equations that models anti-inflammatory cytokines (CA) are given by Eq. 7.

$$\begin{cases} \frac{\partial CA}{\partial t} = -\mu_{CA}CA + (\beta_{CA|MR}.MR.ND + \beta_{CA|MA}.MA).(1 - CA/caInf) + \\ \qquad +D_{CA}\Delta CA \\ CA(x,0) = 0, \frac{\partial CA(.,t)}{\partial n}|_{\partial\Omega} = 0 \end{cases} \tag{7}$$

The term $\mu_{CA}CA$ models the anti-inflammatory cytokine decay, where μ_{CA} is the decay rate. The term $\beta_{CA|MR}.MR.ND$ models the anti-inflammatory cytokine production by the resting macrophages in the presence of apoptotic neutrophils, where $\beta_{CA|MR}$ is the rate of the production. The term $\beta_{CA|MA}.MA$ models the anti-inflammatory cytokine production by active macrophages, where $\beta_{CA|MA}$ is the rate of this production. The saturation of this production is calculated by equation $(1 - CA/caInf)$, where $caInf$ is the maximum concentration of anti-inflammatory cytokine into the tissue. The term $D_{CA}\Delta CA$ models the anti-inflammatory cytokine diffusion, where D_{CA} is the diffusion coefficient.

3.5 Protein Granules

Protein granules (G) are represented by the set of equations presented in Eq. 8.

$$\begin{cases} \frac{\partial G}{\partial t} = -\mu_G G + \beta_{G|N}.sourceN.(1 - G/gInf) + D_G\Delta G \\ G(x,y,z,0) = 0, \frac{\partial G(.,.,.,t)}{\partial n}|_{\partial\Omega} = 0 \end{cases} \tag{8}$$

The term $\mu_G G$ models the protein granules decay, where μ_G is the decay rate. The term $\beta_{G|N}.sourceN$ models the production of the protein granules by the neutrophils that extravasate from the blood into inflamed tissue, where $\beta_{G|N}$ is the rate of this production. The saturation of the production of protein granules is calculated by equation $(1 - G/gInf)$, where $gInf$ is the maximum concentration of protein granules. The term $D_G\Delta G$ models the protein granules diffusion, where D_G is the diffusion coefficient.

4 Computational Model

The numerical method employed to implement the mathematical model was the Finite Difference Method [17], a method commonly used in the numeric discretization of PDEs. The Finite Difference Method is a method of resolution of differential equations that is based on the approximation of derivatives with finite difference.

Below we have an example of a finite difference operator used in the discretization of the Laplace operator that simulates the diffusion phenomenon in 3D:

$$
\begin{aligned}
D_O\left(\frac{\partial^2 O(x,y,z)}{\partial x^2} + \frac{\partial^2 O(x,y,z)}{\partial y^2} + \frac{\partial^2 O(x,y,z)}{\partial z^2}\right) \approx \\
D_O * ((o[x+1,y,z] - 2 * o[x,y,z] + o[x-1,y,z])/deltaX^2)) \\
+D_O * ((o[x,y+1,z] - 2 * o[x,y,z] + o[x,y-1,z])/deltaY^2)) \\
+D_O * ((o[x,y,z+1] - 2 * o[x,y,z] + o[x,y,z-1])/deltaZ^2))
\end{aligned}
\tag{9}
$$

In Eq. 9 O represents the discretization of some types of cells, such as neutrophils, resting and activated macrophages; D_O is the diffusion coefficient of these populations of cells; x, y and z are positions in space; and $deltaX$, $deltaY$ and $deltaZ$ are the space discretization.

In three dimensions, the chemotaxis flux is as follows:

```
//flux at x-axis
if((CH[0][x][y][z]-CH[0][x-1][y][z]) > 0) {
  flux_left = -(CH[0][x][y][z]-CH[0][x-1][y][z]) * O[0][x-1][y][z]/deltaX;
} else {
  flux_left = -(CH[0][x][y][z]-CH[0][x-1][y][z]) * O[0][x][y][z]/deltaX;
}
if(CH[0][x+1][y][z]-CH[0][x][y][z] > 0) {
  flux_right = (CH[0][x+1][y][z]-CH[0][x][y][z]) * O[0][x][y][z]/deltaX;
} else {
  flux_right = (CH[0][x+1][y][z]-CH[0][x][y][z]) * O[0][x+1][y][z]/deltaX;
}
fluxX = (flux_left + flux_right)/deltaX;

//flux at y-axis
if(CH[0][x][y][z]-CH[0][x][y-1][z] > 0) {
  flux_left = -(CH[0][x][y][z]-CH[0][x][y-1][z]) * O[0][x][y-1][z]/deltaY;
} else {
  flux_left = -(CH[0][x][y][z]-CH[0][x][y-1][z]) * O[0][x][y][z]/deltaY;
}
if(CH[0][x][y+1][z]-CH[0][x][y][z] > 0) {
  flux_right = (CH[0][x][y+1][z]-CH[0][x][y][z]) * O[0][x][y][z]/deltaY;
} else {
  flux_right = (CH[0][x][y+1][z]-CH[0][x][y][z]) * O[0][x][y+1][z]/deltaY;
}
fluxY = (flux_left + flux_right)/deltaY;

//flux at z-axis
if(CH[0][x][y][z]-CH[0][x][y][z-1] > 0) {
  flux_left = -(CH[0][x][y][z]-CH[0][x][y][z-1]) * O[0][x][y][z-1]/deltaZ;
} else {
  flux_left = -(CH[0][x][y][z]-CH[0][x][y][z-1]) * O[0][x][y][z]/deltaZ;
}
if(CH[0][x][y][z+1]-CH[0][x][y][z] > 0) {
  flux_right = (CH[0][x][y][z+1]-CH[0][x][y][z]) * O[0][x][y][z]/deltaZ;
} else {
  flux_right = (CH[0][x][y][z+1]-CH[0][x][y][z]) * O[0][x][y][z+1]/deltaZ;
}
fluxZ = (flux_left + flux_right)/deltaZ;
```

In this code fragment, *ch* represents the discretization of the pro-inflammatory cytokine; O represents the discretization of some types of cells; x, y and z are the positions in space; and $deltaX$, $deltaY$ and $deltaZ$ are the spatial discretization. The final result of the evaluation of the chemotaxis is:

$$-\nabla.(\chi_O O \nabla CH) \approx -\chi_O * (fluxX + fluxY + fluxZ) \tag{10}$$

Where the speed of the movement is given by the term ∇CH and χ_O is the chemotaxis rate of the correspondent population of cells. This value is then used to choose between two schemes of finite differences: forward or backward.

Table 1. Initial Conditions. All values are estimated and represent the number of cells.

Parameter	**Value and Position**
A_0	$100, \quad 0 \leq x \leq 1 \quad \& \quad 0 \leq y \leq 1 \quad \& \quad 0.9 \leq z \leq 1$
MR_0	$1, \quad 0 \leq x \leq 1 \quad \& \quad 0 \leq y \leq 1 \quad \& \quad 0 \leq z \leq 1$
MA_0	$0, \quad 0 \leq x \leq 1 \quad \& \quad 0 \leq y \leq 1 \quad \& \quad 0 \leq z \leq 1$
N_0	$0, \quad 0 \leq x \leq 1 \quad \& \quad 0 \leq y \leq 1 \quad \& \quad 0 \leq z \leq 1$
ND_0	$0, \quad 0 \leq x \leq 1 \quad \& \quad 0 \leq y \leq 1 \quad \& \quad 0 \leq z \leq 1$
CH_0	$0, \quad 0 \leq x \leq 1 \quad \& \quad 0 \leq y \leq 1 \quad \& \quad 0 \leq z \leq 1$
G_0	$0, \quad 0 \leq x \leq 1 \quad \& \quad 0 \leq y \leq 1 \quad \& \quad 0 \leq z \leq 1$
CA_0	$0, \quad 0 \leq x \leq 1 \quad \& \quad 0 \leq y \leq 1 \quad \& \quad 0 \leq z \leq 1$

Table 2. Time and Space Discretization

Parameter	**Size**	**Discretization**
Time	$1day$, symbolized by 10^6 iterations	$\delta T = 0.000001$
X-axis	$1mm$, symbolized by 11 points	$\delta X = 0.1$
Y-axis	$1mm$, symbolized by 11 points	$\delta Y = 0.1$
Z-axis	$1mm$, symbolized by 11 points	$\delta Z = 0.1$

Tables 1 and 2 present the initial conditions, the time discretization (δT) and the space discretization (δX, δY and δZ). All the parameters used in our simulations can be found at Table 3. Some values were estimated based on values found in the literature.

Table 3. The complete set of parameters used in the simulation

Parameter	Value	Unit	Reference
$keqch$ and keq_g	1	cell	estimated
θ_{CA}	1	1/cell	estimated
$Pmax$	11.4	1/day	estimated based on [18]
$Pmin$	0.0001	1/day	estimated
$NmaxTissue$	8	cell	estimated
$MrPmax$ and $MrPmax_g$	0.1 and 0.5	1/day	estimated
$MrPmin$ and $MrPmin_g$	0.01 and 0	1/day	estimated
$MrmaxTissue$	6	cell	estimated
$maActivationRate$	0.1	1/cell.day	estimated
μ_A and μ_{MR}	0 and 0.033	1/day	[19]
$\lambda_{N\|A}$	0.55	1/cell.day	[19]
$\lambda_{MA\|A}$	0.8	1/cell.day	[19]
D_A	0.2	mm^2/day	estimated
D_{MR}	0.00432	mm^2/day	estimated
X_{MR}	0.0036	mm^2/day	estimated
μ_{MA}	0.07	1/day	[19]
D_{MA}	0.003	mm^2/day	estimated
X_{MA}	0.00432	mm^2/day	estimated
μ_N and μ_{CH}	3.43 and 7	1/day	estimated
$\lambda_{A\|N}$	0.55	1/cell.day	[19]
D_N	0.012096	mm^2/day	[20]
X_N	0.0144	mm^2/day	[21]
$\lambda_{ND\|MA}$	2.6	1/cell.day	[19]
D_{ND}	0.000000144	mm^2/day	[19]
$\beta_{CH\|N}$	1	1/cell.day	estimated
$\beta_{CH\|MA}$	0.8	1/cell.day	estimated
D_{CH}	0.009216	mm^2/day	[19]
μ_G and μ_{CA}	5 and 4	1/day	estimated
$\beta_{G\|N}$	0.6	1/day	estimated
D_G	0.009216	mm^2/day	estimated
$\beta_{CA\|MR}$	1.5	1/cell.day	estimated
$\beta_{CA\|MA}$	1.5	1/day	estimated
D_{CA}	0.009216	mm^2/day	estimated
$caInf$ and $chInf$	3.6	cell	estimated based on [6]
$gInf$	3.1	cell	estimated

5 Numerical Results

This section presents the numerical results of the simulation. The simulator was build using the C programming language. A numerical library, such as NAG[22], could be used to solve the PDEs. However, we decided to implement the numerical method to solve PDEs because a) we have the possibility to parallelize the code; b) most of the numerical libraries offer few functions that are suitable to our problem; and c) functions offered by such numerical libraries are hard to use because arguments supplied to functions must be in a specific format.

Due to the lack of space, the results obtained from the simulations for some types of cells are not presented. Figures 1, 2 and 3 depict the spatial and temporal distribution of antigens, resting macrophages and neutrophils, respectively, in a 1 mm^3 tissue.

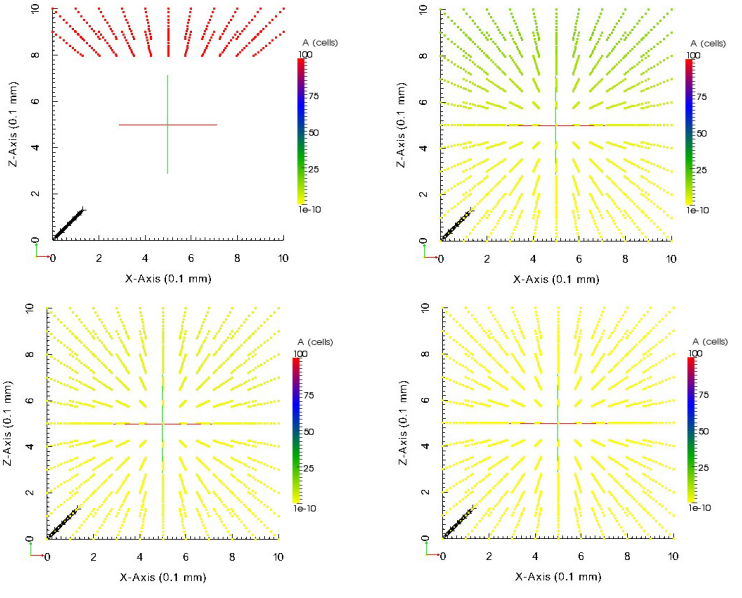

Fig. 1. Spatial and temporal distribution of antigens. Top left is the initial distribution, top right shows its distribution after 6 hours, bottom left after 12 hours and bottom right after 24 hours.

It can be observed that, at first, the number of resting macrophages decreases because they become active to attack LPS. Citokynes are produced and attract neutrophils to the place of infection. These neutrophils that are attracted also contributes to produce even more cytokines in the locations of the tissue where the LPS are more concentrated, resulting in a vigorous and rapid immune response. LPS are eliminated between 6 and 12 hours. After this, it can be observed that the number of resting macrophages start to increase again, while the number of neutrophils start to decrease.

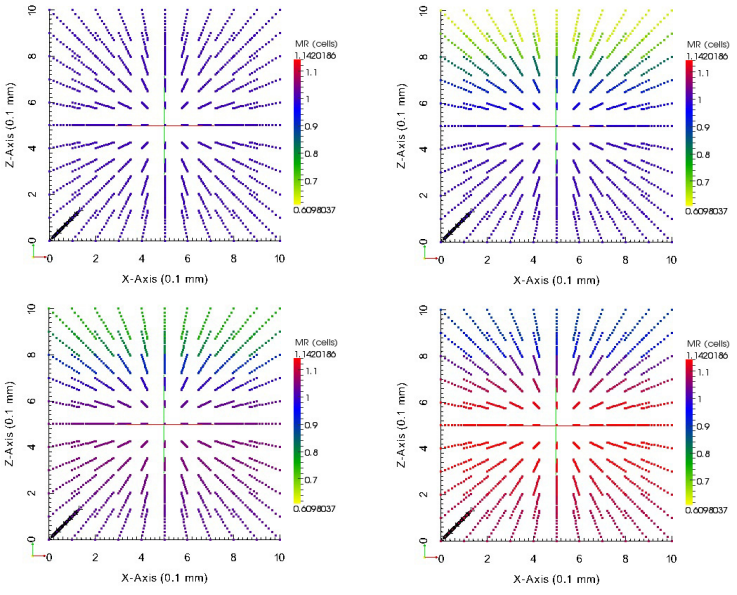

Fig. 2. Spatial and temporal distribution of resting macrophages. Top left is the initial distribution, top right shows its distribution after 6 hours, bottom left after 12 hours and bottom right after 24 hours.

6 Parallel Implementation

The long computational cost of the sequential implementation of the simulator leads the development of a parallel version the code using General-purpose Graphics Processing Units (GPGPUs). GPGPUs were chosen because of their ability to process many streams simultaneously. The present section describes the GPU-based version of the implemented code.

6.1 CUDA

NVIDIA's CUDA (Compute Unified Device Architecture)[23] is a massively parallel high-performance computing platform on GPGPUs. CUDA includes C software development tools and libraries to hide the GPGPU hardware from programmers.

In order to run an application, the programmer must create a parallel function called kernel. A kernel is a function callable from the CPU and executed on the GPU simultaneously by many threads. Each thread is run by a stream processor. They are grouped into blocks of threads or just blocks. The blocks can be one-, two- or three-dimensional. A set of blocks of threads form a grid, that can be one- or two-dimensional. When the CPU calls the kernel, it must specify how

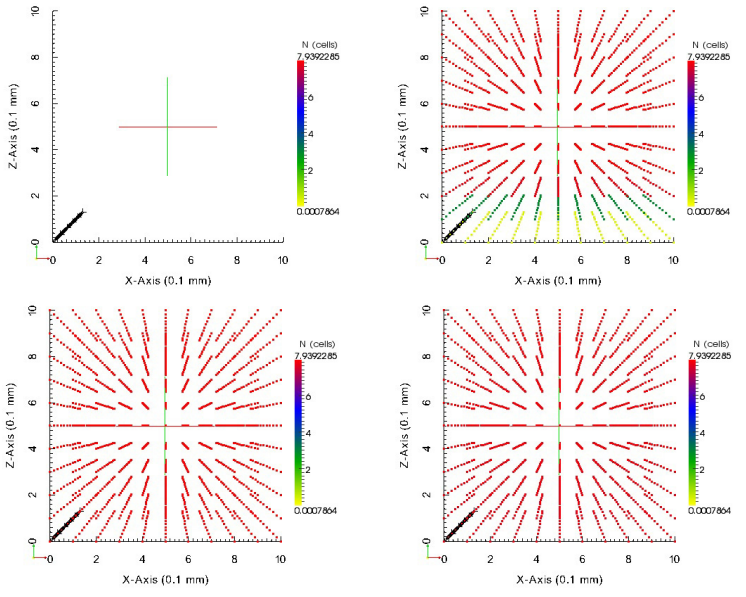

Fig. 3. Spatial and temporal distribution of neutrophils. Top left is the initial distribution, top right shows its distribution after 6 hours, bottom left after 12 hours and bottom right after 24 hours.

many threads will be created at runtime. The syntax that specifies the number of threads that will be created to execute a kernel is formally known as the execution configuration, and is flexible to support CUDA's hierarchy of threads, blocks of threads, and grids of blocks. Since all threads in a grid execute the same code, a unique set of identification numbers is used to distinguish threads and to define the appropriate portion of the data they must process. These threads are organized into a two-level hierarchy composed by blocks and grids and two unique coordinates, called *blockId* and *threadId*, are assigned to them by the CUDA runtime system. These two built-in variables can be accessed within the kernel functions and they return the appropriate values that identify a thread.

Some steps must be followed to use the GPU: a) the device must be initialized; b)memory must be allocated in the GPU and data transferred to it; c) the kernel is called. After the kernel have finished, results are transferred back to the CPU.

6.2 Parallel Version

In the parallel version of the code, each thread is responsible for calculating the complete set of PDEs for each single point of the tissue's space. Therefore, for each point (x, y, z) of the discretized space, there is a thread responsible for the computation of the PDEs. During the computation, the access to data produced

by neighbors threads is necessary. To avoid the use of synchronization, a buffer was implemented to allow that a thread, at time *t*, gets access to data produced by its neighbors at the time *t-1*. The use of a buffer is necessary because a programmer can not synchronize threads that execute in distinct blocks. Besides, the synchronization cost would be prohibitive. No race condition occurs because data being produced in time *t* are accessed just by the thread that is producing it. The buffer is implemented in such a way that there are two values associated for each point (x, y, z) of a given population of cells. One buffer entry is the data produced in time *t-1*, while the other one is data being produced in time *t*. These two buffer entries change their meaning at each time step, in order to avoid copy of data.

In order to store the values for each population of cells in each point of the space, an unidimensional vector was allocated in both CPU and GPU memories. Its length is equal to 8, which are the number of populations, times the number of positions in the tissue.

7 Experimental Evaluation

In this section, we present the speedups obtained with the parallel versions of our code. Both the sequential and parallel implementations have been tested on a dual Intel Xeon E5620 processors each with 4 cores, so 8 physical cores are available. Each core with 64 KB cache L1 and 256 KB L2 and Hyper-threading (HT) which gives the support to 16 simultaneous threads per processor. This machine has a Tesla M2050 GPU, with 448 cores and 2.6 GB of global memory. *gcc* 4.1.2 was used to compile the sequential version of the code, while *nvcc* release 3.2 was used to compile the parallel version. The execution times obtained by all versions of the code were measured 5 times and the standard deviation was lower than 0.13%. Each execution of the code was measured using the Linux *time* application.

The speedup factor was used to evaluate gains obtained by the parallel version of the code over the sequential one. The acceleration can be calculated employing the following Equation 11:

$$S(p) = \frac{t_s}{t_p} \tag{11}$$

where t_s is sequential execution time and t_p is parallel execution time with p processors.

In order to evaluate the performance gains obtained by the parallel version of the code, a tissue of volume equals to 64 mm^3 was used in the parallel experiments to simulate one day of infection (about one million of interactions). This tissue has a total of $64,000$ points. The speedups are presented in Table 4.

Table 4. Speedup obtained by the CUDA parallel version of the code

Version	Runtime average (s)	Standard deviation	Speedup
Sequential	69,727.68	0.13 %	-
Parallel	970.84	0.06 %	71.82

8 Conclusion

This work presented a three-dimensional mathematical and computational model of the innate immune system. The simulation of one day of infection takes about 20 hours on a sequential machine. This long simulation time leads the development of a parallel version of the code. The CUDA version has achieved an speedup of about 72 times over its sequential counterpart. As future work, we plan to employ multiple GPU devices to increase the application speedup. The use of multiple GPU devices allows the allocation of more threads to compute the equations. The innate immune model will be extended to include more cells, such as Natural Killers and Dendritic Cells, and other substances, such as the proteins of the Complement System.

Acknowledgment. The authors would like to thank the Brazilian agencies CAPES, CNPq, FAPEMIG, FINEP and UFJF.

References

1. Pigozzo, A.B., Macedo, G.C., dos Santos, R.W., Lobosco, M.: Implementation of a Computational Model of the Innate Immune System. In: Liò, P., Nicosia, G., Stibor, T. (eds.) ICARIS 2011. LNCS, vol. 6825, pp. 95–107. Springer, Heidelberg (2011)
2. Pigozzo, A., Macedo, G., Weber, R., Lobosco, M.: On the computational modelling of the innate immune system. BMC Bioinformatics (2012) (Submitted, review in progress)
3. Pigozzo, A.B., Lobosco, M., dos Santos, R.W.: Parallel implementation of a computational model of the his using openmp and mpi. In: International Symposium on Computer Architecture and High Performance Computing Workshops, pp. 67–72. IEEE Computer Society (2010)
4. Opal, S.M., DePalo, V.A.: Anti-inflammatory cytokines. Chest 117(4), 1162–1172 (2000)
5. Fiorentino, D., Zlotnik, A., Mosmann, T., Howard, M., O'Garra, A.: Il-10 inhibits cytokine production by activated macrophages. The Journal of Immunology 147(11), 3815–3822 (1991)
6. de Waal Malefyt, R., Abrams, J., Bennett, B., Figdor, C., de Vries, J.: Interleukin 10(il-10) inhibits cytokine synthesis by human monocytes: an autoregulatory role of il-10 produced by monocytes. J. Exp. Med. 174(5), 1209–1220 (1991)

7. Cassatella, M.A., Meda, L., Bonora, S., Ceska, M., Constantin, G.: Interleukin 10 (il-10) inhibits the release of proinflammatory cytokines from human polymorphonuclear leukocytes. evidence for an autocrine role of tumor necrosis factor and il-1 beta in mediating the production of il-8 triggered by lipopolysaccharide. The Journal of Experimental Medicine 178(6), 2207–2211 (1993)
8. Marie, C., Pitton, C., Fitting, C., Cavaillon, J.M.: Regulation by anti-inflammatory cytokines (il-4, il-io, il-13, tgf)of interleukin-8 production by lps and/or tnf-activated human polymorphonuclear cells. Mediators of Inflammation 5, 334–340 (1996)
9. Kennedy, A., DeLeo, F.: Neutrophil apoptosis and the resolution of infection. Immunologic Research 43, 25–61 (2009), 10.1007/s12026-008-8049-6
10. Lucas, M., Stuart, L., Zhang, A., Hodivala-Dilke, K., Febbraio, M., Silverstein, R., Savill, J., Lacy-Hulbert, A.: Requirements for apoptotic cell contact in regulation of macrophage responses. J. Immunol. 177(6), 4047–4054 (2006)
11. Voll, R.E., Herrmann, M., Roth, E.A., Stach, C., Kalden, J.R., Girkontaite, I.: Immunosuppressive effects of apoptotic cells. Nature 390(6658), 350–351 (1997)
12. Fachada, N.: Agent-based simulation of the immune system. Master's thesis, Instituto Superior Tcnico de Lisboa (2008)
13. Cohen, I.R.: Modeling immune behavior for experimentalists. Immunological Reviews 216(1), 232–236 (2007)
14. Moore, K.W., de Waal Malefyt, R., Coffman, R.L., O'Garra, A.: Interleukin-10 and the interleukin-10 receptor. Annual Review of Immunology 19(1), 683–765 (2001)
15. Borregaard, N., Cowland, J.B.: Granules of the human neutrophilic polymorphonuclear leukocyte. Blood 10, 3503–3521 (1997)
16. Goutelle, S., Maurin, M., Rougier, F., Barbaut, X., Bourguignon, L., Ducher, M., Maire, P.: The hill equation: a review of its capabilities in pharmacological modelling. Fundamental & Clinical Pharmacology 22(6), 633–648 (2008)
17. LeVeque, R.J.: Finite Difference Methods for Ordinary and Partial Differential Equations. Society for Industrial and Applied Mathematics (2007)
18. Price, T., Ochs, H., Gershoni-Baruch, R., Harlan, J., Etzioni, A.: In vivo neutrophil and lymphocyte function studies in a patient with leukocyte adhesion deficiency type ii. Blood 84(5), 1635–1639 (1994)
19. Su, B., Zhou, W., Dorman, K.S., Jones, D.E.: Mathematical modelling of immune response in tissues. Computational and Mathematical Methods in Medicine: An Interdisciplinary Journal of Mathematical, Theoretical and Clinical Aspects of Medicine 10, 1748–6718 (2009)
20. Felder, S., Kam, Z.: Human neutrophil motility: Time-dependent three-dimensional shape and granule diffusion. Cell Motility and the Cytoskeleton 28(4), 285–302 (1994)
21. Chettibi, S., Lawrence, A., Young, J., Lawrence, P., Stevenson, R.: Dispersive locomotion of human neutrophils in response to a steroid-induced factor from monocytes. J. Cell Sci. 107(11), 3173–3181 (1994)
22. Pennington, S.V., Berzins, M.: New nag library software for first-order partial differential equations. ACM Trans. Math. Softw. 20(1), 63–99 (1994)
23. Kirk, D., Hwu, W.: Massively Parallel Processors: A Hands-on Approach. Morgan Kaufmann (2010)